Methylated H3K4, a Transcription-Associated Histone Modification, Is Involved in the DNA Damage Response Pathway

David Faucher, Raymund J. Wellinger*

Department of Microbiology and Infectious Diseases, Faculty of Medicine, Université de Sherbrooke, Sherbrooke, Québec, Canada

Abstract

Eukaryotic genomes are associated with a number of proteins such as histones that constitute chromatin. Post-translational histone modifications are associated with regulatory aspects executed by chromatin and all transactions on genomic DNA are dependent on them. Thus, it will be relevant to understand how histone modifications affect genome functions. Here we show that the mono ubiquitylation of histone H2B and the tri-methylation of histone H3 on lysine 4 (H3K4me3), both known for their involvement in transcription, are also important for a proper response of budding yeast cells to DNA damaging agents and the passage through S-phase. Cells that cannot methylate H3K4 display a defect in double-strand break (DSB) repair by non-homologous end joining. Furthermore, if such cells incur DNA damage or encounter a stress during replication, they very rapidly lose viability, underscoring the functional importance of the modification. Remarkably, the Set1p methyltransferase as well as the H3K4me3 mark become detectable on a newly created DSB. This recruitment of Set1p to the DSB is dependent on the presence of the RSC complex, arguing for a contribution in the ensuing DNA damage repair process. Taken together, our results demonstrate that Set1p and its substrate H3K4me3, which has been reported to be important for the transcription of active genes, also plays an important role in genome stability of yeast cells. Given the high degree of conservation for the methyltransferase and the histone mark in a broad variety of organisms, these results could have similar implications for genome stability mechanisms in vertebrate and mammalian cells.

Introduction

Genomes of living organisms are continuously exposed to DNA damaging agents such as ultraviolet light, ionizing radiation, reactive oxygen intermediates or other chemical mutagens. These agents can cause mutations and ultimately genome instability. For mammalian cells, it has been estimated that endogenous DNA damage occurs at a rate of 10 000 events per day [1]. Of the observed DNA damages, double strand breaks (DSBs) potentially are the most deleterious and therefore must be efficiently detected and repaired. Eukaryotic cells have developed multiple mechanisms in order to respond adequately to such DNA damage and many of those mechanisms are highly conserved [1–3]. In *Saccharomyces cerevisiae*, the appearance of DSBs triggers DNA damage checkpoints which ultimately lead to arrest of the cell cycle [4]. It is thought that this controlled arrest provides sufficient time for the repair machinery to locate the break and properly repair the lesion by one of two major DSB repair pathways. During S and G2/M phases of the cell cycle, DSBs are primarily repaired by homologous recombination (HR) between sister chromatids or homologous chromosomes. In G1 and if there is no homology available elsewhere, non-homologous end joining (NHEJ) can repair DSBs by direct religation of the break. This pathway however is much more discrete in yeast.

The repair of DNA damage has to occur in the context of chromatin and its local composition, modification and configuration does affect DNA repair [5]. Therefore, DNA compaction by chromatin must be tightly and locally regulated in order to allow access of protein complexes associated with DNA transactions. There are two key mechanisms to regulate relative opening and closing of chromatin for example at a site of DNA damage: chromatin remodelling and histone modifications [6–9]. Chromatin remodelling is achieved by dedicated complexes that hydrolyse ATP in order to remove or mobilize nucleosomes in the area of a DSB (SNF2-type ATPases, see [10,11], for reviews). It is thought that this creates a discrete change in the general chromatin architecture that allows more efficient repair [12]. In budding yeast, a number of chromatin remodelers such as Ino80, RSC, Swi/Snf and Swr1 have been associated with the DSB repair process [8,13–18]. These complexes are rapidly recruited to a DSB and some directly interact with the DNA damage repair machinery.

Modifying histone proteins is a second possibility by which cells can change the chromatin at the site of a DSB [6,9,19]. Histones can be the target of a number of covalent modifications, including acetylation, phosphorylation, methylation, ubiquitination, ADP-ribosylation and sumolyation [9,19]. An example of such a modification is the phosphorylation of histone H2A on residue

Author Summary

Over the last years, it has become evident that chromatin plays a crucial role in a variety of cellular processes. Insights into the tight regulation of chromatin opening and closing via chromatin remodelers, as well as post-translational modifications of proteins making up chromatin, have revealed new facets on the mechanisms used by cells in order to replicate, transcribe, or repair their DNA. In this report, we describe the involvement of a transcription-linked histone modification, methylation of histone H3 on lysine 4, in the DNA damage repair process. We discovered that in addition to its presence at promoters of highly transcribed genes, H3K4me3 is recruited to sites of newly created double-stranded breaks. Moreover, the results show that this recruitment is dependent on a chromatin remodeler, namely the RSC complex. Cells lacking this histone modification display similar defects as those devoid of the RSC complex; i.e. a significant decrease in the repair of DNA breaks by the non-homologous end-joining repair pathway and a difficulty to survive in presence of replication stresses. All these observations highlight the importance of this conserved histone modification, given that it is involved in a variety of mechanisms affecting genome function.

S129 which can be documented very rapidly after the formation of even a single DSB [20]. A histone modification involved in a number of chromatin-regulated pathways in yeast is the ubiquitination of histone H2B on lysine 123 (H2BK123ub) [21]. This modification in fact is a necessary prerequisite for the methylation on K4, K36 and K79 of histone H3 [22–24]. Methylation of K79 by Dot1p has been associated with DNA damage resistance and the ability to induce the DNA damage checkpoint [25,26]. Tri-methylation of H3K4 (H3K4me3) by Set1p on the other hand is found in the 5′-area of many highly transcribed genes and is thought to be a marker for recent transcriptional activity ([27–29], reviewed in [30]). A possible association of Set1p with DNA repair has been invoked ([26,31], reviewed in [32]), but no definitive evidence has emerged. Furthermore, it has been shown that the Dot1p-mediated effect on DNA repair is distinct and separate from any possible Set1p effect [25].

Here, we show that H3K4 methylation by Set1p indeed is an important event for efficient DNA DSB repair. Consistent with previous results, Bre1p- and Lge1p-dependent ubiquitylation of H2BK123 is also required. The results show that Set1p as well as H3K4me3 accumulate at an inducible DNA DSB and the appearance of Set1p is dependent on the presence of the RSC-complex. In addition, set1Δ cells are deficient in the NHEJ repair pathway and appear to be impaired in traversing S-phase in the presence of replication stress. These data thus show that H3K4 methylation is associated with modulating chromatin at the site of DNA damage and significantly broadens the functional importance of this modification.

Results

A strong synthetic interaction between LGE1/BRE1 or SET1 and the MRX complex

In an attempt to find potential new regulators of telomere homeostasis, a synthetic genetic array experiment was performed using mre11Δ and rad50Δ mutants as baits and looking for lethality or growth delay in double mutants [33]. The screen yielded, lge1Δ (YPL055C) as displaying a synthetic slow growth phenotype at 23°C when combined with the deletion of any member of the MRE11/RAD50/XRS2 (MRX) complex (Figure 1A). Lge1p has been shown to interact genetically and biochemically with the RING finger domain protein Bre1p [23,34]. Yeast Lge1p and Bre1p thus have been suggested to form an ubiquitin ligase complex (E3) that binds to Rad6p (E2) in order to monoubiquitylate histone H2B [23,35]. Given these interactions, we asked if BRE1 would display the same genetic interaction with MRX as LGE1. Indeed, double mutant bre1Δ MRXΔ cells display a very similar synthetic slow growth phenotype as lge1Δ MRX (Δ cells (Figure 1A). Interestingly, both lge1Δ tel1Δ and bre1Δ tel1Δ mutants do not display such synthetic slow growth (Figure 1A), suggesting that for this particular phenotype, TEL1 is in a different genetic pathway than MRX. This contrasts with the fact the MRX complex and TEL1 have been shown to be in the same genetic pathway with respect to telomere maintenance and DNA damage checkpoints [36,37]. These experiments indicate that both Lge1p and Bre1p act in a genetic pathway parallel to MRX and which is important for normal growth of the cells.

In the course of these genetic analyses, we also discovered that bre1Δ rad50Δ cells were highly sensitive to DNA damaging agents. Both lge1Δ rad50Δ and bre1Δ rad50Δ display dramatically reduced viability when treated with the IR-mimetic drug bleomycin, UV light or the DNA replication inhibitor hydroxyurea (HU) (Figure 1B and data not shown). Note that the conditions used for inducing replication stress or DNA damage were relatively mild such that in these experiments, even rad52Δ or rad50Δ cells display only a minor growth defect as compared to a wild type strain (see Figure 1B, for example). Consistent with the observed growth properties at 23°C, a hyper-sensitivity to DNA damage was not observed in bre1Δ tel1 (Δ double-mutants (Figure 1C). These data thus suggest that in the absence of MRX, DNA damage survival is dependent on the presence of LGE1 and BRE1.

Previously, the BRE1 and LGE1 genes had been characterized as key players for modulation of gene transcription in yeast (reviewed in [21]). These genes, together with RAD6, are required for mono-ubiquitylation of histone H2B on the lysine residue 123 which in turn is required for the methylation of histone H3 on lysines 4 and 79 [21,23,35]. Set1p and Dot1p are the two methyltransferases that methylate, respectively, histone H3K4 and H3K79. Given this known cascade of histone modifications, the downstream effect of the absence of Bre1p or Lge1p could be dependent on this histone modification pathway or occur via a new and histone-independent pathway. We therefore tested whether an absence of histone modifications also sensitizes MRXΔ cells to DNA damage. Cells harbouring a combination of rad50Δ and a mutant allele of histone H2B that cannot be ubiquitinated (H2BK123R) are as sensitive to bleomycin as bre1Δ MRXΔ or lge1Δ MRXΔ cells (Figure 1D). Therefore, the DSB sensitivity of bre1Δ MRXΔ cells can be explained by the incapacity of the cells to ubiquitinate histone H2B on lysine 123. Further, in MRXΔ cells, neither the deletion of DOT1 nor the mutation of its substrate histone H3K79 sensitizes the cells to bleomycin (Figure 1E and 1F). On the other hand, deletion of the methyltransferase SET1 or the presence of a H3 allele that cannot be methylated on lysine 4, H3K4R, combined with an absence of the MRX complex lead to an indistinguishable sensitivity as observed in lge1Δ/bre1Δ MRXΔ cells (Figure 1E and 1F). BRE2 and SPP1 have also been reported to be required for methylation of H3K4, albeit to varying degrees for the bi-methylated and tri-methylated forms [38,39]. However, in our hands only a deletion of BRE2 but not that of SPP1 lead to a complete lack of H3K4me3 (Figure S1A, S1B, and S1C). Remarkably, the sensitivity of the respective double mutants (i.e.
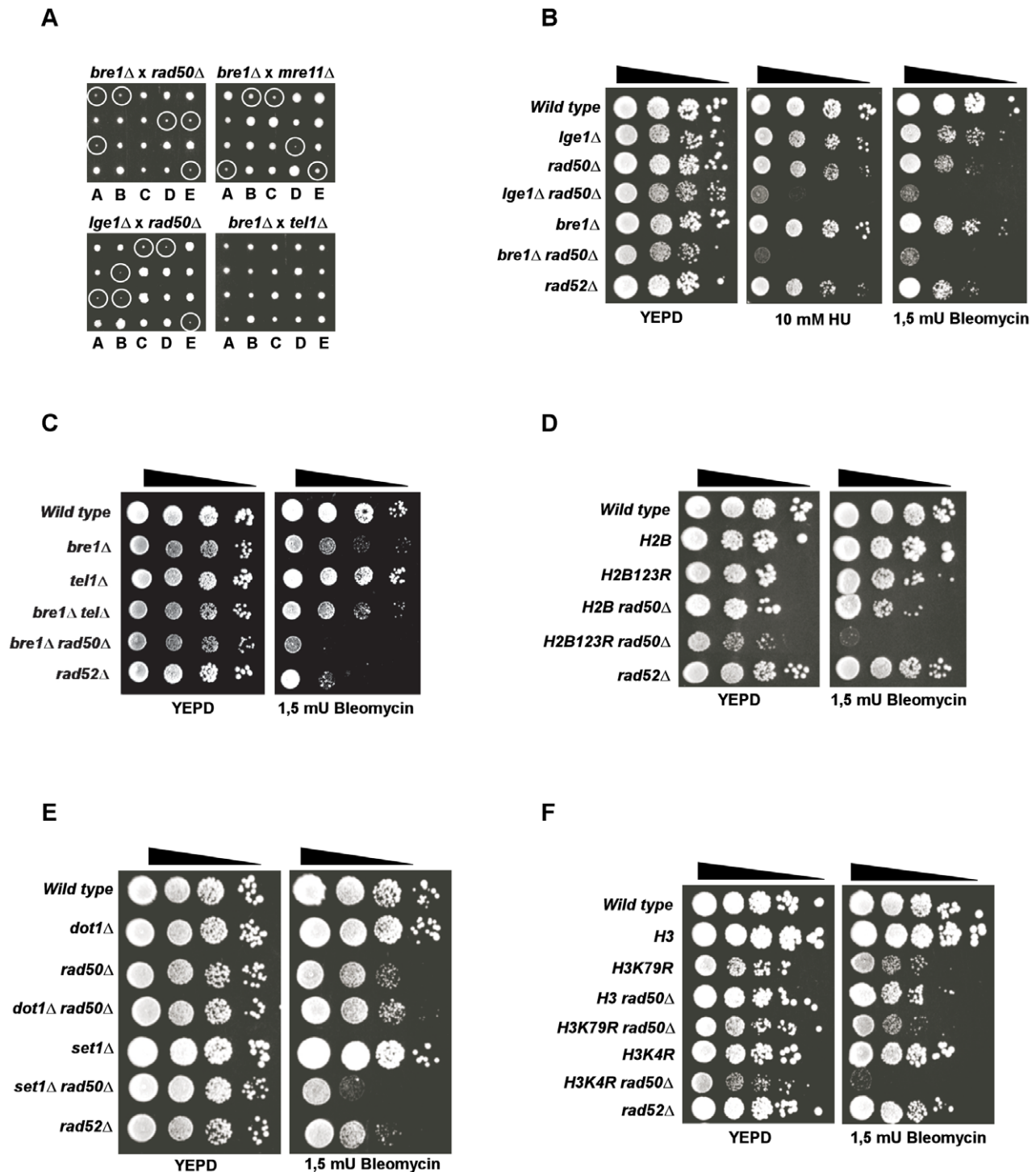
Figure 1. Genetic interactions between a histone modification pathway and the MRX complex. (A) Tetrad analysis of spores derived from diploids micro-dissected on YEPD plates and allowed to grow for 3 days at 23°C. Circled colonies are double mutants. Diploids DFY001, DFY002, DFY004 and DFY005 respectively, were used as starting strains. (B–F) Serial ten-fold dilution growth tests of exponentially growing cultures on plates with the indicated compounds. YEPD: control plates without drug; (B) Growth of cells with a deletion of members of the Ubiquitin-Ligase complex in combination with a deletion of *RAD50* (spores derived from diploids DFY002 and DFY007); (C) Spot dilution test of *bre1Δ tel1Δ* double mutant cells on plates containing the indicated concentration of Bleomycin (right) or no drug (left, spores were derived from DFY005); (D) Growth of cells with a mutant that cannot be mono-ubiquitylated (H2BK123R) (strains YZS276, YZS246, DFY008, DFY009 and MT0-73); (E) Growth of cells with deletions of *DOT1* or *SET1* genes in combination with absence of *RAD50* (spores derived from diploids DFY010 and DFY012); and (F) Growth of cells with a mutant histone H3 that cannot be methylated (H3K79R or H3K4R) and combined with an absence of *RAD50* (strains YZS267, DFY013, DFY015, DFY016, DFY017 and DFY018).

doi:10.1371/journal.pgen.1001082.g001

bre2Δ/rad50Δ or *spp1Δ/rad50Δ*) to Bleomycin correlated with this finding: a *bre2Δ/rad50Δ* strain in which H3K4me3 levels are below detection as in a *set1Δ/rad50Δ* strain is exquisitely sensitive, whereas the *spp1Δ/rad50Δ* strain is not (Figure S1A, S1B, and S1C). Finally and as expected, *set1Δ* and H3K4R appear to act in the same genetic pathway (see below Figure 5A). We conclude that in the absence of the MRX complex, Set1p and the methylation of H3K4 are important for the survival of the cells in presence of DNA damage.

Set1p-mediated H3K4 methylation is involved in DSB repair by NHEJ

Because cells lacking both *SET1* and the MRX complex are very sensitive to DSB, we decided to verify which of the main DSB repair pathways, homologous recombination (HR) and non-homologous end joining (NHEJ) were affected in cells lacking Set1p. In order to test whether *SET1* indeed is involved in NHEJ, *set1Δ*-cells were analyzed for NHEJ efficiency. A plasmid religation assay was performed using a transformation assay with linearized vector DNA. The circularization efficiency in strains deleted for *YKU70* and *DNL4* was about 5% of that obtained in *wt* cells, confirming their importance in this assay (Figure 2A). Notably, the absence of *SET1* also caused an important decrease in the capacity of cells to complete NHEJ and to religate the plasmid: overall religation efficiency in these cells was reduced to about 30% of that seen in *wt* (Figure 2A).

In addition, we used strain JKM179 harbouring the HO endonuclease controlled by a galactose-inducible promoter. In this strain, the natural donor sequences usually used for homologous recombination after the HO recognition site is cut are deleted from the genome. Therefore, upon induction of expression of the HO endonuclease, these cells can only repair the DSB at the mating type locus by NHEJ [40]. Deletion of *SET1* in this strain background and exposing the strains to galactose resulted in a significant decrease of the viability of the cells as compared to *wt*, albeit not to the level of sensitivity of *yku70Δ* cells that display the expected dramatic decrease in viability due to an almost complete absence of NHEJ (Figure 2B).

To confirm the involvement of *SET1* in the NHEJ repair pathway, we also used a strain that contains a cassette flanked by two *HO* cleavage sites [41,42]. Following *HO* endonuclease induction by addition of galactose to growth media, both *HO* cleavage sites are cut and given the absence of homology in the rest of the genome for sequences on either side of the cassette, the gap had to be repaired by NHEJ (see Figure S2A). When grown in liquid culture containing galactose as carbon source and thus continuously induced HO cleavage, strains with a deletion of *SET1* display a similar extended lag-time before growth recovery as strains deleted for *YKU70* or *DNL4* (Figure 2C). In these conditions, growth recovery could be dependent on two different mechanisms: error-prone NHEJ or MMEJ (Microhomology-mediated end joining). In the case of wild type and *set1Δ* cells, growth is restored via the error-prone NHEJ during which the HO-recognition site must be lost such the HO enzyme does not continuously induce the DSB. However cells completely unable to carry out NHEJ (cells harbouring *yku70Δ* and *dnl4Δ* alleles), bypass the continuous HO cleavage via MMEJ using small stretches of homology in order to perform DSB repair [43]. The results obtained with the liquid culture assays were paralleled by results obtained with the same strain, but using a colony color assay for error-free and error-prone assays ([41,42], Figure S2B). Given the dependence of NHEJ on the presence of the Yku-proteins at the DNA break, it was possible that in Set1p-lacking cells, the binding of Yku to the break was impaired. We used chromatin immunoprecipitation (ChIP) experiments with a myc-tagged Yku80p to assess Yku binding at the induced break at the *MAT*-locus and the results show significantly reduced association of Yku with the breaks (Figure 2D). In parallel experiments, the same experimental setup with gal-induced expression of the HO endonuclease was used to assess HO-cutting efficiencies of the HO-sites flanking the *ADE2*-cassette and on a plasmid borne *MAT*-locus (see Figure S2A, S2C, and S2D). The results confirm that these induced cleavages occur at indistinguishable rates when wild-type and *set1Δ* cells are compared (Figure S2C and S2D), a result that is also consistent with the sensitivity to HO-induced DSB of the *set1Δ* cells (Figure 2C). These experiments establish that in *set1Δ* cells, the efficiency of NHEJ, in particular of the error-prone branch of this repair pathway, is impaired when compared to wild type cells. Consistent with this conclusion, Yku-binding at an induced DSB is reduced.

Abolition of the two DSB repair pathways (NHEJ and HR) at the same time leads to synergetic sensitivity of the cells to DNA damaging agents. As an example, this can be observed for cells harbouring deletions of both *DNL4* and *RAD52* and in which NHEJ and HR are lacking ([44], Figure 2E). Thus, we combined deletions of *DNL4* and/or *RAD52* with *set1Δ* and tested the sensitivity of the resulting cells to bleomycin. At the bleomycin concentration used in this experiment, neither *set1Δ* nor *dnl4Δ* single mutants display a significant sensitivity and grow as well as wild type cells. As mentioned above, *rad52Δ* cells were only mildly affected (Figure 2E). The *set1Δ dnl4Δ* double mutant cells also were not sensitive to this bleomycin concentration, which is consistent with the possibility that these two genes act in the same genetic pathway. Yet, double mutant *set1Δ rad52Δ* and particularly the triple mutant *set1Δ dnl4Δ rad52Δ* displayed a sensitivity to DSB that is even higher than that of *dnl4Δ rad52Δ* cells (Figure 2E). However, as assessed by a Q-PCR method, we could not discern in *set1Δ* cells a major defect in homologous recombination mediated mating-type switching (Figure S3), which is consistent with the observation that in the presence of the HR machinery, *set1Δ* cells are not very sensitive to radiomimetic drugs (Figure 1E and Figure 2E). These results confirm that *SET1* is involved in the NHEJ repair pathway and suggests that it may even have additional roles in maintaining genome stability, particularly in the presence of DNA damage.
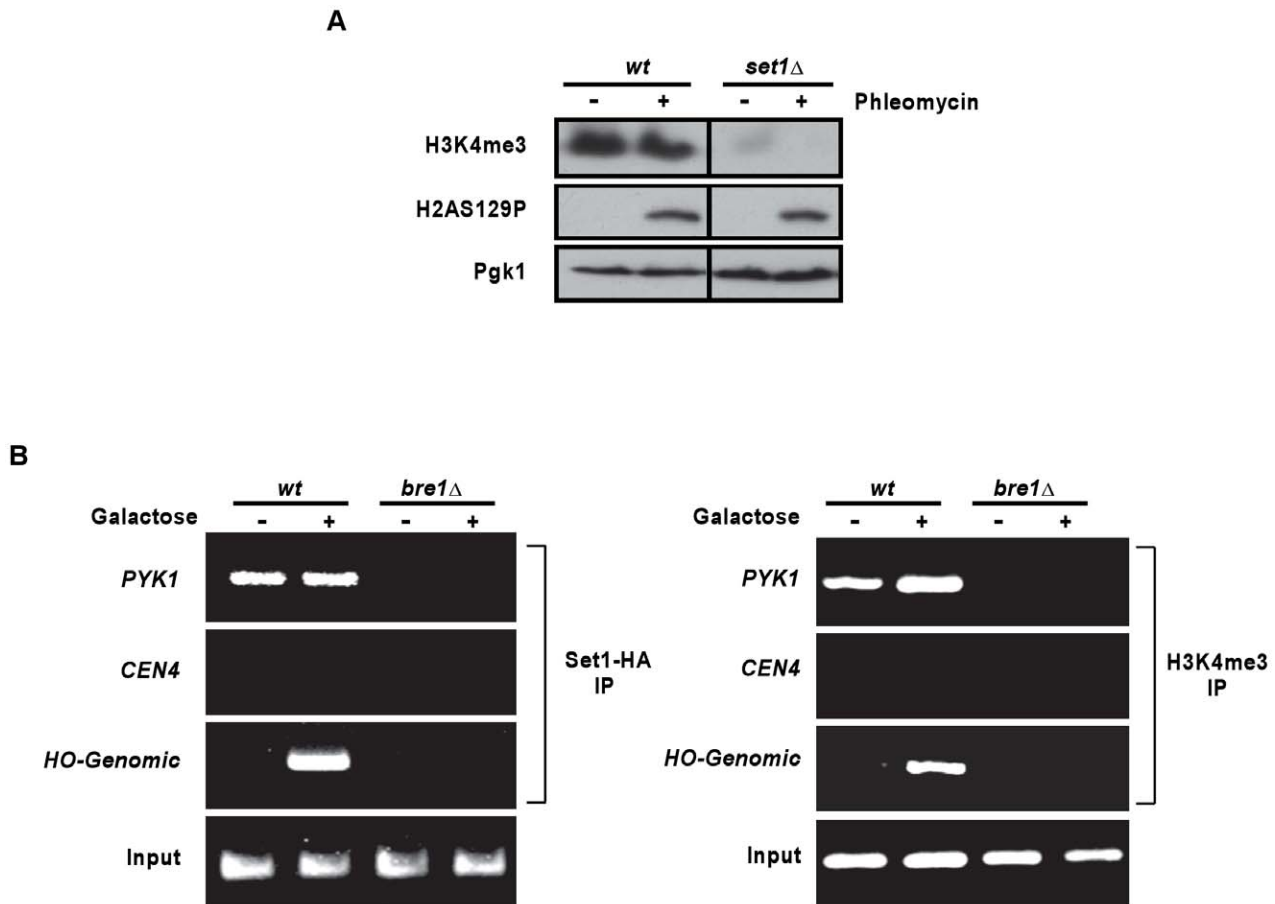
Recruitment of the SET1 methyltransferase and detection of H3K4me3 at newly created DSBs

It is well documented that H3K4 trimethylation is present on H3 in nucleosomes at a majority of promoters and 5′ parts of active genes [27,28,30,32,45,46]. Based on the observations above highlighting the importance of H3K4me3 in DNA damage repair processes, we asked whether or not this histone modification could be induced at the site of DNA damage. First, we tested whether there was a global increase in H3K4me3 in chromatin following DNA damage. Exposure to phleomycin of wild type cells did not result in an increase in the global amount of H3K4me3 (Figure 3A and Figure S4). Moreover, the levels of phosphorylated H2AS129 did not significantly vary between *set1Δ* cells and wild type cells, indicating that this part of the chromatin modification at a DNA damage site seems to be by en large properly activated in this mutant (Figure 3A). The failure to be able to detect an increase in H3K4me3 after DNA damage induction by phleomycin could be explained by an already relatively high level of H3K4me3 that is associated with active transcription. A slight further increase of that global level in this experiment may simply be undetectable by western blotting, even if high doses of phleomycin were used (Figure S4). We therefore turned to an assay that verifies the
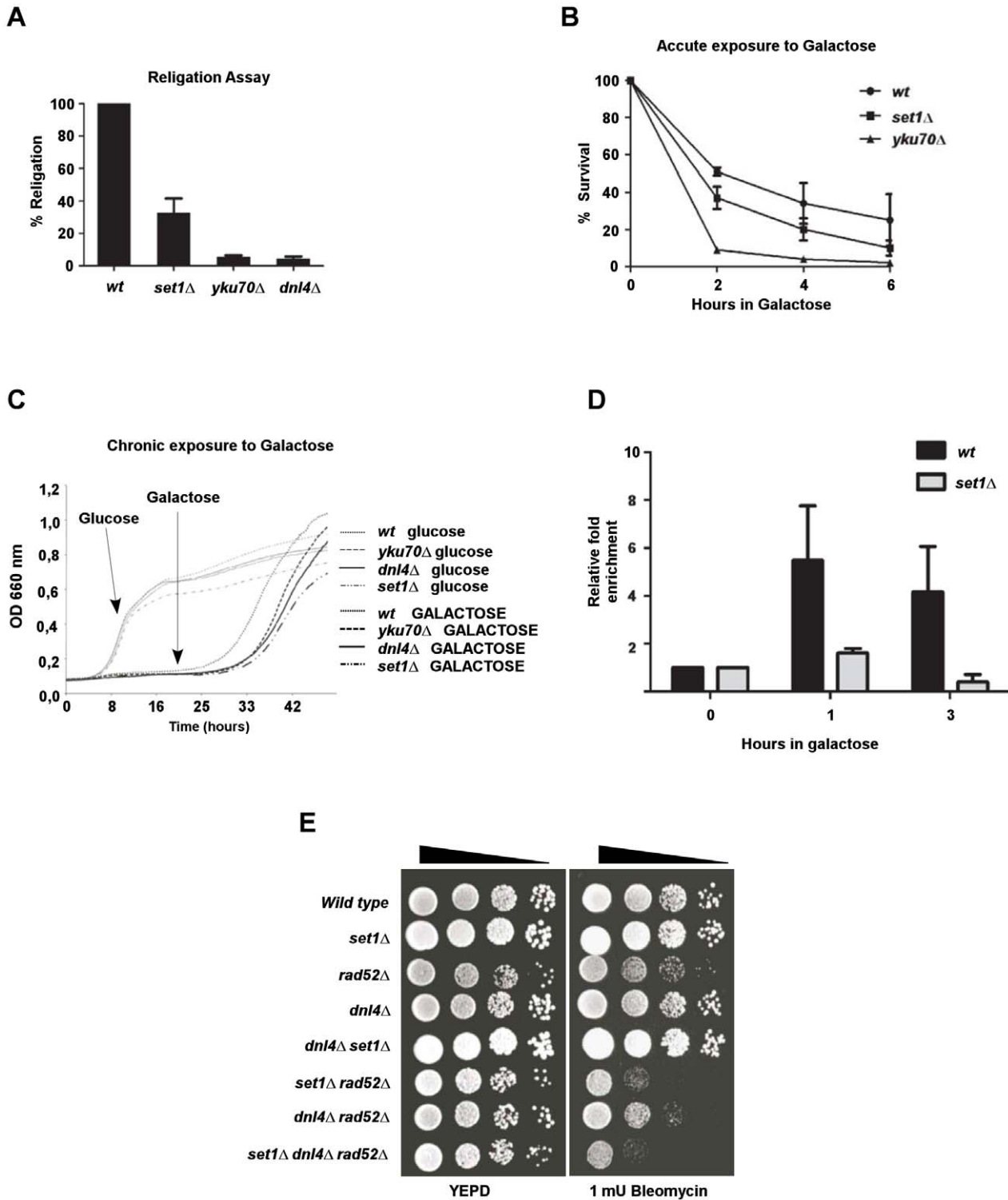
Figure 2. The *LGE1-BRE1-SET1* histone modification pathway is involved in DSB repair by non-homologous end joining (NHEJ). (A) *Set1Δ* cells display a deficiency in a plasmid religation assay. Linearized plasmid pRS316 was transformed into wild type cells (*wt*, YW1276), *set1Δ* (DFY021), *yku70Δ* (YW1283) or *dnl4Δ* cells (DFY022). Overall percentage of religation was calculated using transformation efficiency normalization. (B) Survival of *wt* (JKM179), *set1Δ* (DFY023) or *yku70Δ* cells (JKM181) following induction of a DSB. Cells were held in galactose media for the indicated time and then plated on glucose medium, shutting off HO endonuclease expression. In these strains, the induced DSB at the mating type locus can only be repaired by NHEJ. (C) Growth curves of *wt* (YW1276), *set1Δ* (DFY021), *yku70Δ* (YW1283), and *dnl4Δ* cells (DFY022) exposed to a constant expression of HO endonuclease. (D) Recruitment of Yku80-myc protein to an induced DSB site in *wt* (DFY048) and *set1Δ* (DFY049) cells. DSB induction was performed for 1 and 3 hours, ChIP performed with an anti-myc antibody and immunoprecipitated DNA quantified by Q-PCR. Fold enrichment is normalized to non-induced cells (glucose) set as 1. (E) Sensitivity to DNA damage of cells harbouring deletions of genes affecting, respectively, NHEJ (*DNL4*) or homologous recombination (*RAD52*) when combined with a deletion of *SET1*. Strains used were spores of DFY020.
doi:10.1371/journal.pgen.1001082.g002

Figure 3. Site-specific recruitment of the Set1p methyltransferase and detection of H3K4me3 at a DSB. (A) Western blot of proteins derived from *wild type* and *set1*Δ cells that were treated (+) or not (−) with phleomycin. Top: Tri-methylated H3K4 was detected with an antibody against H3K4me3; middle: detection of phosphorylated H2AS129 as a positive control for phleomycin treatment; and bottom: anti-Pgk1p antibody as a loading control. Strains used were *wt* DFY024 and *set1*ΔDFY026). (B) Left: Recruitment of HA-tagged Set1p methyltransferase to the mating type locus was tested by ChIP analysis using an anti-HA antibody. HO endonuclease was expressed for 90 min in G1-arrested *wt* (DFY027) or *bre1*Δ cells (DFY028). DNA was extracted from immunoprecipitates and PCR amplified with specific primers adjacent to the HO cleavage site, primers in the promoter region of the highly expressed gene *PYK1*, or primers specific for the transcriptionally repressed *CEN4* locus. Right: Same experiment as in left panel, except that instead of the anti-HA antibody, an antibody specific for H3K4me3 was used for the immunoprecipitation.
doi:10.1371/journal.pgen.1001082.g003

potential recruitment of the Set1p methyltransferase to a specific DSB by (ChIP) analysis. Fortunately, Set1p and H3K4me3 are virtually absent from the endogenous HO cut site located at the mating type locus ([23]; Figure 3B). In our setting, the HO endonuclease was induced in wild type or *bre1*Δ cells, both also harbouring a functional Set1p-HA allele. Chromatin was immunoprecipitated with an anti-HA antibody [23] or a H3K4me3-specific antibody. As expected, irrespective of whether HO is induced or not, Set1p and H3K4me3 can be detected on the promoter of *PYK1*, a gene known to be highly expressed throughout the cell cycle (Figure 3B, [23]). On the other hand, neither was detectable at the centromere of chromosome 4, an area that is transcriptionally repressed in a constitutive fashion. Finally, when the cells were grown in glucose and in the absence of the HO endonuclease, Set1p and H3K4me3 were not detected at the MAT locus, while after induction of HO by galactose; both became detectable at this same locus (Figure 3B). Formally, it was possible that addition of galactose to growth media leads to a transcription mediated recruitment of Set1p. However, as assessed by Northern blotting and RT-QPCR, the level of Mat**a**1-RNA transcribed at the *MAT* locus in these cells did not vary

significantly between glucose and galactose-grown cells (Figure S5A and S5B). Furthermore, we also assessed occurrence of H3K4me3 at *MAT* in a strain containing a *MAT* locus that is not susceptible to HO-cutting (*MATa-inc*) by ChIP and no increase of the H3 modification could be detected (Figure S5C). These results therefore show that Set1p associates with a newly created DSB *in vivo* and induces *de novo* trimethylation of histone H3 at the site.

Intra-S retention of set1Δ mutants following exposure to DNA damaging agents

In order to verify whether cell cycle transitions that are controlled by checkpoint activation are normal in mutants where H3K4 trimethylation was abrogated, we analyzed cell cycle progression of cells after exposure to DSB inducing agents (Figure 4A). Cells were arrested in G1, treated with 10 μg/ml of phleomycin for 90 min, then washed two times with sterile water in order to remove all traces of the DNA damaging agent as well as the α-mating factor and finally released into fresh media lacking drugs. Compared to untreated wild type cells, phleomycin exposed cells were delayed for 30 min before entry into S-phase, as expected (Figure 4A). However, once the G1 checkpoint delay
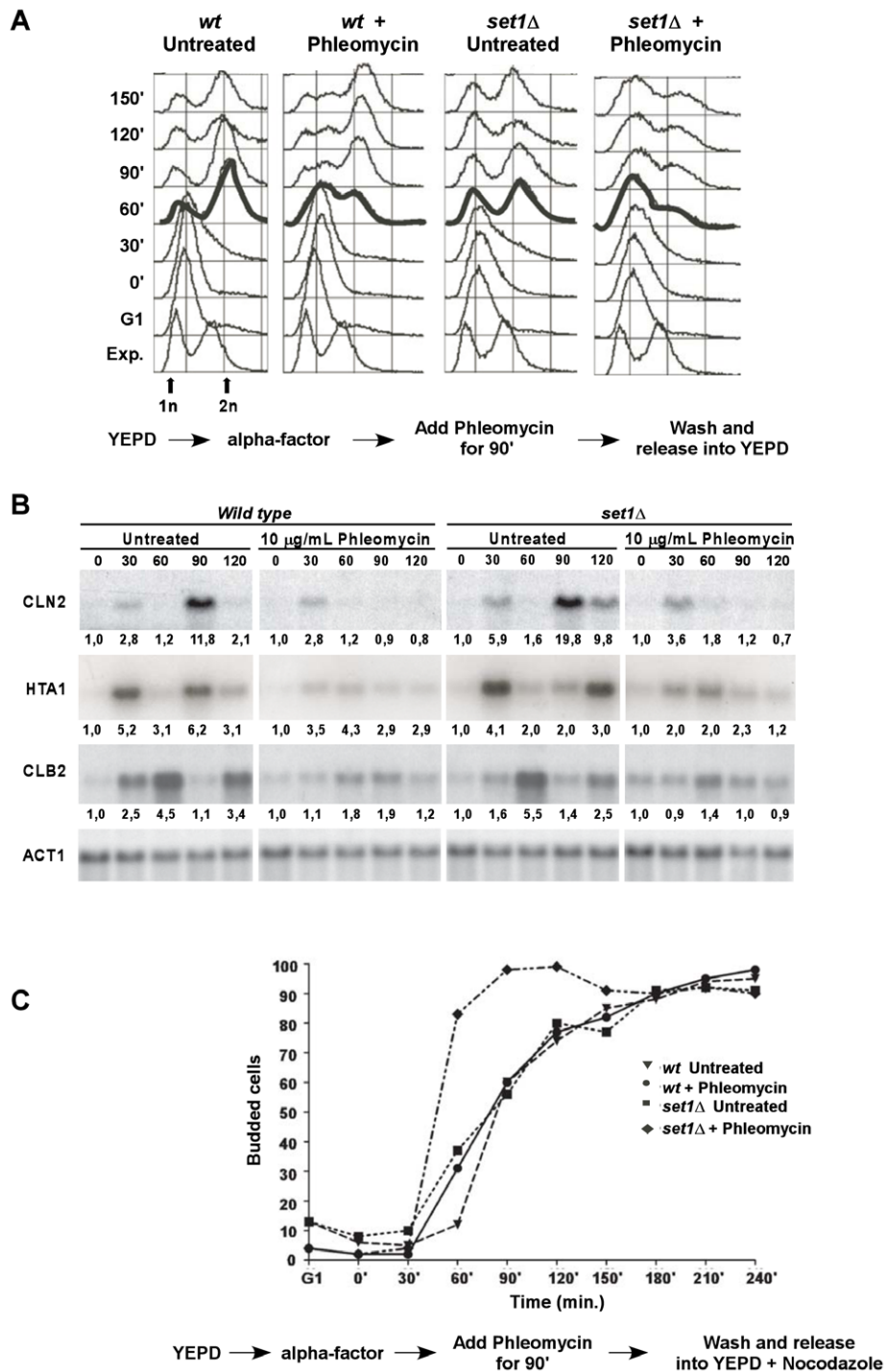
Figure 4. Set1Δ cells exposed to DNA damage in G1 are retained in S-phase. (A) *wt* (DFY024) and *set1Δ* cells (DFY026) were arrested in G1 phase of the cell cycle and exposed to phleomycin (see experimental scheme at bottom). Cells were then released and cell cycle progression was monitored by flow cytometry of samples at regular intervals. Time 0 min represents the release of cells into rich medium immediately following the phleomycin treatment. (B) In a separate release experiment, northern blot analysis was performed in order to confirm the expression of cell-cycle specific mRNAs: Cln2 for G1, Hta1 for S-phase and Clb2 for G2/M specific RNA expression. A probe specific for the Act1-mRNA was used as a non-varying control (bottom). The number below each lane indicates the change of the signal intensity for the particular RNA; the level at time 0 was set as 1. (C) Budding indexes of *wt* (DFY024) and *set1Δ* cells (DFY026) subjected to a cell synchrony and release experiment as outlined below the curves. Note that the final media did contain Nocodazole to prevent cells to traverse multiple cycles and that explains why the indexes stay high at the end of the experiment.

doi:10.1371/journal.pgen.1001082.g004

overcome, the majority of cells resumed their cell cycle and went on to the G2/M phase. Untreated set1Δ-cells did also display a slight delay in S-phase entry, but the cells did resume cycling (Figure 4B). Exposure of the G1-synchronized mutant set1Δ to the same concentration of DNA damaging agent as above resulted in a retention of the majority of the cells in G1 or early S phase of the cell cycle (Figure 4A). These cells appeared not to resume cycling as they failed to reach the G2/M phases of the cycle (Figure 4B).

From these FACS analyses, it was not possible conclusively to deduce whether treated set1Δ cells remained arrested in G1 or actually did enter but could not complete S-phase. Therefore, in order to determine more precisely the exact phase of the cell cycle where these cells were arrested, we decided to analyze mRNA expression profiles of the G1/S cyclin Cln2p, the S-phase specific transcript for histone H2A (HTA1) and the G2/M cyclin Clb2p. Aliquots of cells were taken at 30 min intervals after release from the G1-arrest and mRNA was extracted. In untreated samples, both for wild type and set1Δ cells the expected oscillations of the expression of Cln2 or Clb2 RNA through the cell cycle can be observed (Figure 4B, top and third rows). Peak expression levels for these two cyclins are temporally separated and occur at the expected time after G1 release indicating properly cycling cultures. Following exposure to phleomycin, both wild type and mutant cells display an induction of the Cln2 RNA at 30 min whereas Clb2 RNA increases after about 60 min, but there is no detectable mRNA peak at later time points, (Figure 4B). These data are consistent with the FACS profiles as they confirm that such cells do not complete further cell cycles. The expression profiles of the S-phase specific histone H2B mRNA strongly suggest that bleomycin treated set1Δ cells in fact do enter S-phase and are not blocked at the G1/S boundary: Hta1 mRNA is induced at the 30 min time point and remains at an elevated level for about 60 min (Figure 4B). This induction of the Hta1 mRNA strongly suggests actual entry into S and the assessment of budding indexes during a similar experimental protocol supports this notion (Figure 4C). Collectively, these data show that cells lacking Set1p and exposed to DNA damaging agents can enter S-phase but encounter difficulty traversing it.

Evidence for sensitivity of set1Δ cells to replication stresses

The above experiments show that after genotoxic treatments, cells without the ability to introduce the H3K4me3 chromatin mark experience problems in S-phase. One hypothesis that could explain the results is that replication of damaged DNA in set1Δ cells is compromised. Indeed, set1Δ cells and cells expressing H3K4R are sensitive to hydroxyurea, a compound affecting DNA replication, confirming that tri-methylation of H3K4 is important for the passage through S in the presence of genotoxic stress (Figure 5A and 5B). The set1Δ, H3K4R double mutant displays a similar sensitivity as each single mutant, again consistent with the suggestion that they act in the same genetic pathway in terms of HU-sensitivity (Figure 5A). Next, we analyzed S-phase progression in wild type and set1Δ cells after a transient exposure to HU. Cells were arrested in G1, then released into S in the presence of 200 mM HU and finally HU was washed out and cells released into rich media containing Nocodazole (Figure 5C). In wild type cells, this situation causes some delay in S-phase resumption (data not shown), but after 30 min, most cells resumed and they completed S-phase after 45 min (Figure 5C, left). For set1Δ cells, the progression profile is delayed by about 15 min and many cells have not reached G2 even 90 min after the release (Figure 5C, middle). Another mutant known to enter but incapable to traverse S-phase, arp8Δ, a member of the INO80-complex [8,17,18],

exposed to similar experimental conditions showed a comparable phenotype as set1Δ cells (Figure 5B and data not shown). Furthermore, set1Δ rad52Δ and mrc1Δ rad52Δ cells displayed a very similar sensitivity to exposure to a low dose of bleomycin, while either deletion alone or a combination of set1Δ mrc1Δ did not display any significant sensitivity (Figure 5D). Mrc1p is involved in the activation of the Rad53 kinase during the S-Phase checkpoint [47,48] and also has an independent function in the stabilization of stalled replication forks [49–51]. Moreover, while both set1Δ and yku70Δ cells are compromised in their ability to repair DSBs by NHEJ, only set1Δ-cells, but not yku70Δ cells are sensitive to HU (Figure S6). These experiments strongly suggest that Set1p is important for the passage of cells through S-Phase in presence of DNA damage and replication stress and this effect is at least partially independent of the effect of a set1Δ on NHEJ.

SET1 acts in conjunction with the RSC remodelling complex

The above results show that binding of Set1p and methylation at H3K4 are important events at sites of DNA damage in S-phase. Thus, we speculated that the methylated histone H3 may be important for the subsequently necessary chromatin remodelling and DNA repair activities. Methylated histones can bind or stabilize the association of various proteins that contain bromo-domains, tudor domains alongside chromodomains or plant homeodomain (PHD)-finger motifs [30,52]. Selected yeast candidate genes containing such domains and having the potential to bind H3K4me3 were tested for a genetic interaction with RAD50, similar to the one of the genes in H2BK123ub/H3K4me3 pathway in the presence of DNA damage. Amongst the genes tested in this fashion were CTI6 (SAGA-complex), CHD1 (SAGA and SLIK-complexes), SAS3 and YNG1 (Nua3-complex), EAF3 (Nua4-complex), ISW1, RDH54 and RAD54; none of which showed an interaction comparable to the one of SET1 (Figure 6A for YNG1 as an example). The exceptions in this regard were non-essential members of the yeast RSC remodelling complex, RSC1 and RSC30. When deletions of either of those genes were combined with rad50Δ, the cells displayed a DNA damage sensitivity that was very similar to that of set1Δ rad50Δ cells (Figure 6B and 6C) and rsc2Δ rad50Δ double mutants also showed increased sensitivity, albeit not as dramatic (data not shown). In addition the rsc30Δ set1Δ rad50Δ triple mutant cells were as sensitive as each double mutant, which is consistent with the idea that SET1 and RSC30 act in the same genetic pathway (Figure 6B).

In order to further examine whether cells lacking RSC30 or SET1 behave in a similar fashion, cell cycle synchrony experiments were performed (Figure 5C). Rsc30Δ cells were synchronized in G1, released into a synchronous S-phase in the presence hydroxyurea for 90 min and then released by washing out the drug. As observed for set1Δ cells, rsc30Δ cells experienced an S-phase delay (compare wt and rsc30Δ cells at 45 min after release, Figure 5C). The above experiments thus establish a number of intriguing correlations between the RSC complex and Set1p: they are both associated with newly created DSBs, their absence causes strongly compromised NHEJ and also an increased sensitivity to genotoxic agents if HR is also compromised (Figure 2, Figure 3, Figure 6B, and [13]). We therefore investigated whether the recruitment of Set1p to DSBs was dependent on RSC or vice versa. As already shown above, Set1p localization to an induced DSB at MAT is readily detectable in wt, but abrogated in bre1Δ cells (Figure 3, Figure 6D). In addition, similar to the situation in bre1Δ cells, Set1p recruitment was undetectable in rsc30Δ cells (Figure 6D). This absence of Set1p recruitment to a break was not due to a general absence of the H3K4me3 modification in rsc30Δ
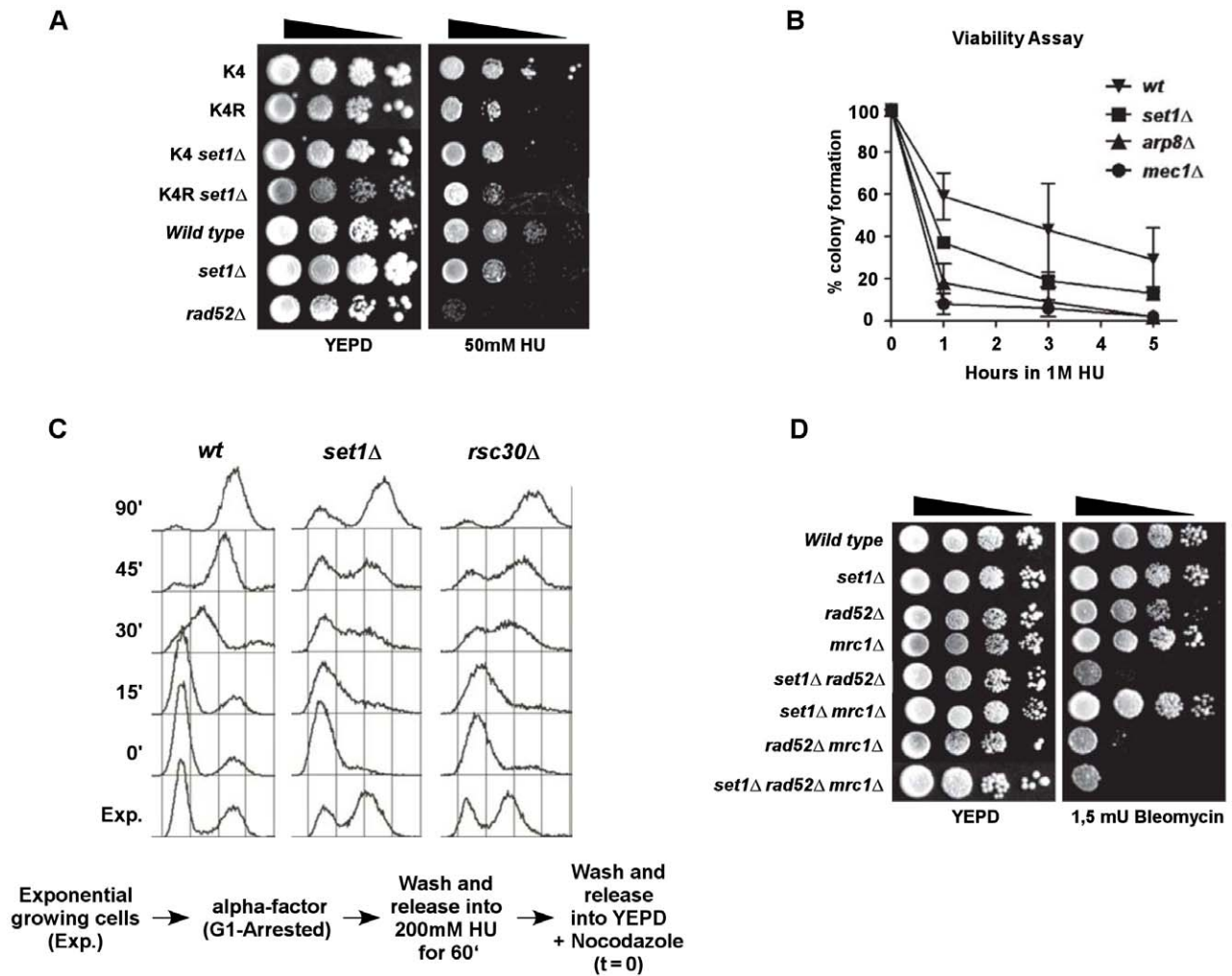
Figure 5. Replication defects in *set1Δ* cells. (A) Serial ten-fold dilution growth test of strains with the relevant genetic setup on plates with 50mM HU. Strains used were YZS267, DFY017, DFY038, DFY039, DFY024, DFY026 and MT0-73. (B) Viability curves of the indicated strains exposed to HU for the indicated time. Strains used were *wt* (DFY024), *set1Δ* (DFY026), *arp8Δ* (DFY030), *mec1Δ* (DFY044). (C) *wt* (DFY024), *set1Δ* (DFY026)or *rsc30Δ* (DFY029) cells were arrested in G1 phase of the cell cycle and released into a synchronous S-phase in the presence of 200 mM HU for 60 min. The HU block was removed by washout and cell cycle progression was analyzed by FACS. Time 0 min represents the release of cells into rich medium plus Nocodazole following the HU treatment. (D) Viability of strains with indicated genotype and derived from strain DFY032 were grown in liquid media and ten-fold serial dilutions were plated onto YEPD control plates or onto a plate containing bleomycin, as indicated.
doi:10.1371/journal.pgen.1001082.g005

cells: as assessed by western blot, the overall H3K4me3 levels remained similar to wild-type in these cells (Figure 6E), suggesting that the H3K4me3 modification associated with highly transcribed areas occurs normally in *rsc30Δ* cells. On the other hand, myc-tagged Sth1p, an essential subunit of the RSC-complex can be detected on DSBs in *wt* and *set1Δ* cells (Figure 6F and data not shown).

In order to verify whether a temporal order of binding of the RSC-complex versus the occurrence of H3K4me3 at a DSB can be established, Sth1p-myc and H3K4me3 were immunoprecipitated at different time intervals after a DSB induction. The results show a time dependent increase for both, peaking at about 40 min after break induction (Figure 7A and 7B), but they don't allow a differentiation in terms of order of appearance. Note that after only 30 min, cleavage efficiency in this strain reached about 60% (Figure 7C).

These results are consistent with the genetic data above (Figure 6B and 6C) and strongly suggest that Set1p recruitment

to a DSB is dependent on the proper function of the RSC-complex.

Discussion

Appropriate regulation of chromatin modifications and chromatin remodelling is essential for efficient transcription, replication and repair of DNA (Reviewed in [21,30]). The results of this study demonstrate that in budding yeast, the methylation of lysine 4 on histone H3 (H3K4me3) is involved in maintaining genome stability. Strains lacking the respective methyltransferase Set1p display three specific phenotypes that support this statement: an impaired ability to recruit the Yku-proteins to a DSB leads to a strongly reduced efficiency of NHEJ (Figure 2), *de novo* Set1p as well as H3K4me3 appearance at a site of an induced DSB (Figure 3), and a difficulty to pass through S-phase in presence of replication stresses (Figure 5). These effects, when combined with an absence of HR lead to a hypersensitivity to DNA-damaging agents (Figure 1, Figure 2, Figure 5, Figure 6). Although these
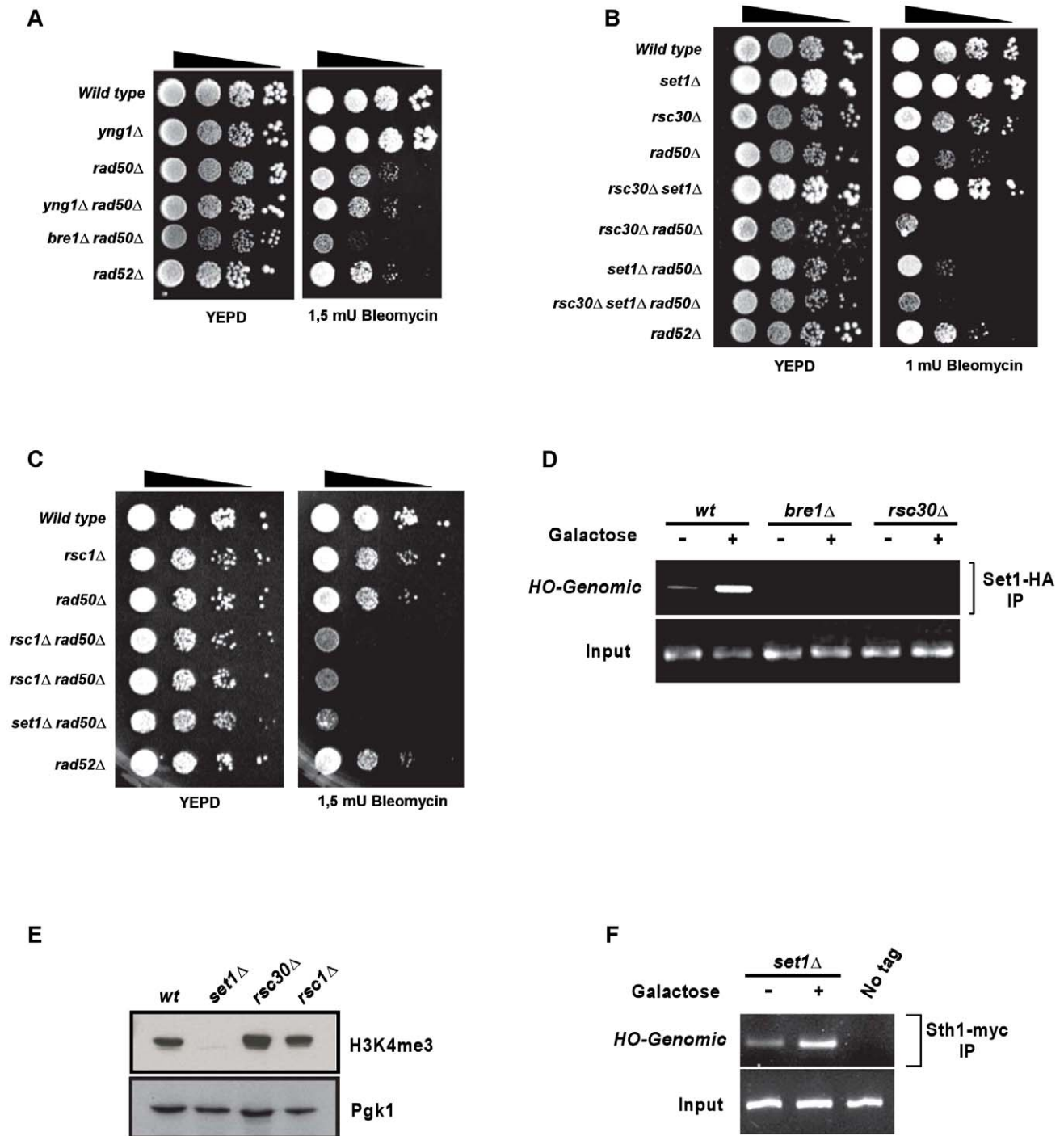
Figure 6. Functional interactions between the RSC complex and *SET1*. (A) Example of a spot dilution - colony viability assay performed to unc subunits *RSC30* in (B) and *RSC1* in (C), in combination with a deletion of *RAD50* and/or *SET1* (spores derived from diploid DFY034 and DFY050 respectively). Serial ten-fold dilution growth tests of exponentially growing cultures on plates containing DNA damaging agent bleomycin. YEPD: control plates without treatment. (D) ChIP experiments assessing the presence of Set1p in *wt* cells (DFY027) or in cells lacking either *BRE1* (DFY028) or *RSC30* (DFY037). (E) Western blot analysis detecting the presence of H3K4me3 in strains harbouring deletions of RSC complex subunit genes. A *set1Δ*– strain serves as negative control and re-hybridization with and anti-Pgk1p antibody was used as a loading control. Strains used were spores of diploid DFY034 and DFY050. (F) ChIP of an essential RSC-component, Sth1p, in cells lacking *SET1*. Strain used was DFY046. ChIP experiments essentially were conducted as described in Figure 3 over genes displaying a similar DNA damage sensitivity enhancement as *set1Δ* in absence of homologous recombination. Note that *yng1Δ* scored here is negative, the *bre1Δ rad50Δ* serves as positive control; strains used are spores of DFY033. (B,C) Growth of cells with a deletion of RSC complex.
doi:10.1371/journal.pgen.1001082.g006
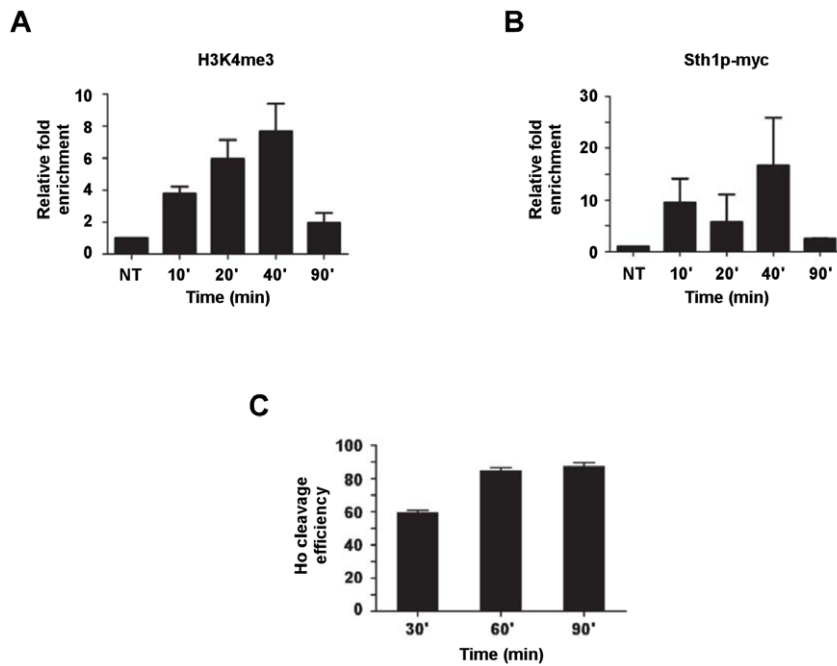
Figure 7. Kinetics of association of H3K4me3 and Sth1p of the RSC complex with an induced DSB. (A,B) ChIP analysis showing the recruitment of H3K4me3 and Sth1p respectively to an induced DSB. Wild-type cells (DFY046) were exposed to galactose for the indicated period in order to induce HO endonuclease. DNA was extracted from immunoprecipitates and analyzed by quantitative PCR using specific primers adjacent to the HO cleavage site. (C) Analysis of the HO cleavage efficiency of cells used for ChIP analysis in (A,B) using Q-PCR. DNA was extracted from cells and Q-PCR with primers overlapping the DSB was performed. Time 0 (glucose) was set to 0% cleavage efficiency.
doi:10.1371/journal.pgen.1001082.g007

observations are paralleled in strains that harbour mutations not allowing ubiquitylation of H2B (Figure 1 and Figure 5), this fact can be explained by the dependence of H3K4 methylation on previous H2B modification [53,54]. However, while H2BK123ub is also required for H3K79 methylation by Dot1p, our data demonstrate that loss of NHEJ-efficiency and the synthetic interactions with MRX are specific to a lack of H3K4me3 and not H3K79me3 (Figure 1). Therefore, the roles played by Set1p in genome stability are quite different from those of the Dot1p methyltransferase [25,26].

This is one of the first reports directly linking H3K4me3, a chromatin modification extensively described for its involvement in marking transcriptionally active loci, to DNA damage repair processes. Given that our results document the *de novo* occurrence of Set1p and the H3K4me3 mark on an induced DSB (Figure 3, Figure 6, Figure 7), we do not think that the effects observed in *set1Δ*-cells are indirect consequences of a change in transcriptional activity. Furthermore, analyses of microarray data of RNA derived from cells harbouring H3K4R, a mutated version of H3 that cannot be methylated, or from cells lacking either of Bre1p, Lge1p, Rad6p and Set1p do not indicate important transcription variation of genes implicated in the DNA damage checkpoints or repair [27,55], M.-A. Osley, personal communication). For example, we could find only 5 genes for which the change was more than 3 fold (increase or decrease) in *lge1Δ*-cells (12 for *bre1Δ* cells) and none of those have a known association with DNA repair (see http://www.utoronto.ca/greenblattlab/BUR.xls). In fact, one study reported a potential increase of repair genes in the absence of Set1p, which would be the opposite effect and could not explain our results [56]. In yeast, there already is evidence for transcription-mark independent functions of Set1p. For example, a number of described subtle cellular phenotypes associated with a *SET1* deletion could be independent of transcriptional changes [57].

More recently, Set1p has been shown to methylate Ipl1p and be involved in chromosome segregation, an effect that is independent of its transcriptional regulation [58]. Finally, recent data does implicate H3K4me3 at sites of active meiotic DSB formation independently of the transcriptional state of the local genomic area [59] and there is one report that links Set1p absence with a deficiency of meiotic S-phase passage, a phenotype similar to the one reported here [60]. Intriguingly, the results on an involvement of Set1p in the regulation of meiosis in yeast have parallels in mouse, where a meiosis-specific H3K4 methyltransferase called Meisetz/*PRDM9* is required for passage through meiosis. Remarkably, meiotic cells in mice lacking Meisetz also display a strong deficiency in DSB repair [61].

Our present hypothesis stipulates that the H3K4me3 chromatin mark is crucial for adequate repair of DSBs, whether they occur accidentally during vegetative growth or are induced in meiosis. For example, if there is a DSB occurring at a specific site in *wt* cells and the H3K4me3 mark is not already present due to transcriptional activity, Set1p is recruited to it in a RSC-dependent fashion (Figure 6). Either concomitant to this recruitment or thereafter, Set1p will induce *de novo* methylation of H3K4 on the nucleosomes surrounding the site (Figure 3). RSC, a SWI/SNF type chromatin remodelling complex, has recently been shown to associate with DSB very early and the preliminary time-coarse data reported here is consistent with those results ([62,63], Figure 7). The results further suggest that this may be true for the occurrence of H3K4me3 too (Figure 7). Similar to what is shown here for the H3K4me3 modification, the recruitment of Mre11p, another protein involved in early recognition DNA damage, is also RSC-dependent [63]. In addition, cells lacking Rsc30p, a non-essential member of RSC, display a number of indistinguishable phenotypes as cells lacking Set1p: an important reduction of NHEJ repair and an increased

sensitivity to chronic exposure to HO endonuclease (Figure 2, [13]) and a marked sensitivity to HU mediated S-phase arrest (Figure 5C). Consistent with a close relationship between RSC, Set1p and the H3K4me3 mark, the respective genes genetically appear to be in the same epistasis group in terms of sensitivity to genotoxic agents (Figure 6). We therefore speculate that nucleosome remodelling by the RSC-complex in conjunction with a relative opening of the chromatin by H3K4 methylation could be important for the ensuing DNA repair mechanisms. However, we failed to be able to demonstrate a direct physical interaction between H3K4me3 and the RSC catalytic subunit Sth1p by co-immunoprecipitation (data not shown).

The results also strongly suggest that an absence of H3K4me3 in cells with damaged DNA causes defects in traversing S-phase; presumably the problems occur when replication forks encounter the site of DNA damage (Figure 5). Recent evidence suggests that the MRX complex plays a variety of roles in damage recognition and checkpoint control during S-phase [64]. Interestingly, some of those MRX functions are independent of the S-phase checkpoint and our data here show that in the presence of DNA damage, cells lacking any of the MRX genes, but not those lacking TEL1, display a high degree of synthetic lethality with a SET1 deletion (Figure 1). It is therefore plausible that MRX and SET1 define two independent pathways that become important for passage through S-phase in the presence of damage, which would explain our synthetic interaction data (Figure 1, Figure 2, Figure 5). A very comparable genetic interaction between the MRX complex and SET1 as the one reported here for budding yeast has also been found in S. pombe [65], which is consistent with the idea that this convergence of two pathways on the DSB repair process is conserved.

Set1p has also been shown to interact with and somehow modify the activity of Mec3p, a conserved checkpoint protein [31]. In addition, in mammalians, there is increasing evidence for an association of tumour suppressor genes with H3K4me3. For example, both the ING1 and ING4 proteins that are associated with DNA repair and cellular transformation bind to H3K4me3 [66,67]. These findings hint to a widespread conservation of this alternate function of the H3K4me3 histone modification brought about by Set1p and homologous proteins in genome stability mechanisms.

This report highlights the complexity of downstream effects due to histone modifications and the occurrence of separate influences on major biological processes such as transcription, DNA replication and DNA damage repair. H3K4me3 generally is accepted as a very important mark in the genome of active promoters and the occurrence of recent transcription [45,46,68]. Here we report our discovery of another, most likely independent role for this chromatin modification: perhaps combined with the recruitment of chromatin remodeling activities it acts as a key player in the pathways governing genome stability in case of DNA damage.

Materials and Methods

Nomenclature

We use the proposed histone modification nomenclature [69]. Trimethylation of the histone H3 on the lysine residue 4 becomes H3K4me3.

Strains and plasmids

All individual S. cerevisiae strains used in this study are listed in Table S1. All strains are isogenic with the S288c background; except strains JKM179, JKM181, YZS276, YZS246, DFY023, yFR016, DFY027, DFY028, DFY035, DFY036, DFY037, DFY046 and DFY047 that were derived from a W303 background. Plasmid YCpHOcut4 has been described before [70].

The strain used for SGA analysis was MLY532 (Matα rad50::NatR can1::MFA1pr-HIS3-MFalpha1pr-LEU2 his3Δ leu2Δ0 ura3Δ0 met15Δ0 lys2Δ0). To create this strain, Y3556 (Matα can1::MFA1pr-HIS3-MFalpha1pr-LEU2 his3Δ leu2Δ0 ura3Δ0 met15Δ0 lys2Δ0) [71] was transformed with a plasmid pJH1032-ad50D-NatR linearized by ClaI. pJH1032-rd50D-NatR was constructed using pJH1032 (former name pNKY1070 [72]) in which the NatR marker gene replaces a Xba1 fragment of RAD50. MLY530 (Matα mre11::NatR can1::MFA1pr-HIS3-MFalpha1pr-LEU2 his3Δ leu2Δ0 ura3Δ0 met15Δ0 lys2Δ0) was created by transforming a BamH1+Xho1 fragment of plasmid pRS313-MRE11d-NatR. To construct pRS313-MRE11d-NatR, MRE1 coding sequences were amplified using oligos CTCGAAAC-TAGTGGATCTCAAACA and CTTGCTATACGAATTCAA-GAGCAAAG harbouring respectively SpeI and EcoRI restriction sites. This fragment was then cloned into pRS313 using the added restriction sites. The resulting plasmid was digested with HpaI and we replaced the excised 2135 bp fragment with a blunted NatR fragment creating pRS313-MRE11d-NatR.

These strains were crossed with the library of nearly 4700 individual haploid strains with the a mating type (background strain BY4741) purchased from Invitrogen Life Technologies. Information is available at the Saccharomyces Deletion project Website. In order to confirm potential hits, we created diploid strains DFY001, DFY002, DFY004 by crossing haploid strains MLY530 and MLY532 with the respective strain from the yeast deletion library.

Strain DFY06 (hht1-hhf1Δ hht2-hhf2Δ rad50Δ::NatR pMS329 (HHT1-HHF1 CEN URA3) was derived from MSY421 (hht1-hhf1Δ hht2-hhf2Δ pMS329 (HHT1-HHF1 CEN URA3) [73]. DFY07 and DFY08 were obtained by a plasmid shuffle introducing plasmids encoding the wild type or mutated versions of histone H3: pZS136 (HHT2-HHF2 CEN TRP1), pZS138 (hht2-K4R-HHF2 CEN TRP1) and pZS138 (hht2-K79R-HHF2 CEN TRP1) [22], obtained from Brian Strahl, UNC-Chapel Hill) with strain DFY06. Transformation of plasmids and DNA into yeast was performed as described [74].

Mutant haploid strains were constructed by replacing the ORF of the targeted gene in parental strain LLY33 (for MT0-73, DFY003, DFY006, DFY011, DFY024, DFY049), YW1276 (DFY021, DFY022), JKM179 (for DFY023), yFR016 (DFY027, DFY028, DFY037), YZS267 (DFY038), DFY017 (DFY039), FT4 Sth1-9myc (DFY047) and a spore of DFY042 (DFY044) with the indicated selection markers using a PCR-mediated gene disruption method [75]. The LLY33 strain was created by micro-dissection of the diploid BY4705 [75]. Strains DFY008, DFY009 and DFY014 were constructed by the integration of a digested fragment derived from the rad50Δ::NatR plasmid into the genomic locus [76]. All strains used in this study had their mutations confirmed by marker segregation and PCR analysis. Strain DFY048 (13XMYC-YKU80) was constructed by adding a C-terminal myc epitope tag to Yku80p using a PCR-based method.

General yeast growth conditions

Cells were grown on standard rich YEPD media containing, if needed, 100 ug/ml of nourseothricin (Clonat, WERNER Bioagents, Germany) or G418 at 150 ug/ml (Sigma). In some cases, synthetic medium YC supplemented with needed amino acids and bases was used. All genetic manipulations were performed as described previously [77,78].

Flow cytometry analysis

Cell synchronizations were performed as published with minor modifications [79,80]. Following a three hours cell synchronization in G1 using α-factor, phleomycin was added to cultures to reach indicated final concentrations and cells were further incubated for 90 min. In order to remove the DNA damaging agent and the α-factor, cells were washed two times with sterile water and resuspended in fresh growth media. At the respective time points of the specific experiments, aliquots were processed for FACS analyses [81] or budded cells were counted using an hemacytometer and percentage of budded cells was calculated as the ratio of budded cells over all cells. For the S-phase release experiments, cells were synchronized in G1 phase for three hours as above, washed two times using sterile water in order to remove the pheromone and resuspended in YEPD media containing 200 mM Hydroxyurea (HU). Cells were left in this media for 60 min, washed again using sterile water and finally resuspended in fresh YEPD media containing Nocodazole for the rest of the experiment. Aliquots were again prepared for FACS analyses at the indicated time points.

Drug sensitivity assays

Cell sensitivity to damaging agents was verified by spot tests on YEPD media containing the indicated concentrations of MMS (Sigma), HU (Sigma) and Bleomycin (BLENOXANE, Bistrol Meyers). Mid-log cultures were spotted in serial 10-fold dilutions and were allowed to grow for 3 to 4 days, before documentation. In later stages of the project, we used Phleomycin in place of Bleomycin as genotoxic agent. In control experiments 0,01 μg/mL of Phleomycin caused the same phenotypes as 1 mU of Bleomycin (data not shown) and the two can be used interchangeably.

For viability experiments after exposure to HU, cells were grown to log phase in YEPD at 30°C and then arrested in G1 with α-factor for three hours. Such synchronized cultures were then washed three times and released into S-phase by resuspension in YEPD to which HU was added to yield a final concentration of 1M. Aliquots of cells were taken after 1, 3 and 5 hours of incubation, cell density determined by counting and aliquots of 2×10^3 cells were plated on YEPD plates. Viability is expressed as the percentage of colonies with respect to the counted cells.

For sensitivity to DNA breaks induced by the HO-endonuclease, JKM179 cells and derivative strains were grown to log phase in YEP-media supplemented with 2% raffinose. Cell concentration was adjusted to 1×10^7 cells/ml in YEPGal media and cells were incubated for 2, 4 or 6 hrs. Cells were then counted and 2×10^3 cells were plated on YEPD media and incubated at 30°C for 2 days. The survival rate of wt cells was determined by dividing the number of colonies obtained by the number of cells plated. All mutant survival rates were compared to the wild type rate which was set to 1.

Plasmid religation assay

In general, the experiment was performed as described previously [40]. The centromeric plasmid pRS316 was digested with the BamHI restriction enzyme and then transformed into yeast cells. The transformation of undigested plasmid done in parallel was used to assess transformation efficiency of each sample. Efficiency of religation was determined by the number of colonies that were able to grow on a media selecting for the marker contained on the plasmid and was normalized by the transformation efficiency for each sample. All religation efficiencies in mutant cells were compared to wild type cells which were set to 100% and yku70Δ and lig4Δ cells were used as controls.

HOSD(+1) NHEJ assay

Essentially, the experiments were done as previously described [41]. Wild type, control strains carrying deletions of genes known to be involved in NHEJ (yku70Δ and lig4Δ) and set1Δ cells were grown in Yc-Met media containing Raffinose as carbon source for 16 hours. For an observation of a chronic exposure to break induction, 4×10^4 cells were incubated in media containing either glucose or galactose and their re-growth characteristics monitored over 48 hrs using an automatic plate incubator and reader (see [82], for details).

Error-prone/Error-Free NHEJ-ratio was obtained by growing cells for 2 days in Yc-Met+Ade +2% raffinose media, followed by a dilution into Yc-complete supplemented with 2% galactose. Cells were allowed to grow for 2 days and then plated at appropriate dilutions onto Yc-complete +2% glucose plates to obtain the total of viable cells, and onto Yc-Ade +2% glucose plates in order to reveal the +2 imprecise NHEJ events. Results were determined by dividing the number of colonies on Yc-Ade plates (imprecise NHEJ) by the total colonies on Yc-complete (all NHEJ events).

Assay for efficiency of homologous recombination

Wild type and set1Δ cells harbouring the YcpHocut4 plasmid were grown for overnight in Yc-Ura media +2% raffinose and diluted to 1×10^7 cells/mL. A first control aliquot (non treated) was removed and cells were re-suspended into Yc-Ura +2% galactose for 1 hour. After this incubation, the second aliquot (galactose) was removed. The remaining culture was washed 3 times in sterile water and resuspended in Yc-Ura +2% glucose. Aliquots were taken at hourly intervals (t = 1 to t = 4). DNA was extracted, quantified and QPCR was performed on all samples in order to analyze the production of the MATα switching product. For both strains, results were normalized to non-treated samples.

Western analyses

Midlog cell cultures were either exposed to 10 μg/ml of Phleomycin for one hour or left untreated and protein extracts were prepared using a modified TCA method [83]. Proteins were separated on an 8% and 15% acrylamid-bisacrylamid gels (ratio 29:1) using standard techniques [84]. Gels were transferred onto a PVDF membrane and treated according to manufacturer's instructions (Perkin Elmer). Anti-H3K4me3 polyclonal antibody was purchased from Abcam (Ab8580) and used at a 1: 5000 dilution. H3K4me0 peptide (a kind gift of Alain Verreault) was used with Ab8580 in order to reduce non-specific binding of the antibody. Anti-H3K4me2 polyclonal antibody was obtained from V. Geli. Polyclonal anti Phospho-H2AS129 (Ab15083) was purchased from Abcam and used at a 1:750 dilution. Signals were detected using horseradish-peroxidase-coupled anti-rabbit secondary antibodies (GE Healthcare) and enhanced chemiluminescence (Perkin Elmer). Monoclonal anti-Pgk1p was obtained from Molecular Probes and used at a 1/20000 dilution.

Northern analyses

RNA extraction and Northern blots were performed as previously described [85]. Cln2 and Hta1 RNAs were detected using radiolabeled probes prepared by a random priming method using the following primers:

Cln2 = TAACAGCAATAACGCAACCA and CCGCAACG-GCGCATTACCT

Hta1 = ATGTCCGGTGGTAAAGGTGG and TCTTGAGA-AGCCTTGGTAGC

Act1 = TCCGGTGATGGTGTTACTCA and ATTCTCAA-AATGGCGTGAGG

Mata1 = CACCGCACAATTCATCATTTGCGT and CTG-GGTAGAGTCTTATTGGCAAGA

RT–QPCR analyses

Synthesis of cDNA was performed using 2 μg of total RNA and SuperScript II Reverse Transcriptase (Invitrogen, Burlington, ON). A gene-specific primer protocol using a "Flap sequence" was used to avoid DNA amplification during subsequent PCR amplification. RNase treated samples were used as negative controls. The cDNA was purified using the QIAgen mini-elute system (Qiagen Inc., Mississauga, ON, Canada). All primers used for RT PCR and the following QPCR are listed in Table S2.

Chromatin ImmunoPrecipitations (ChIP)

DFY027 or DFY028 cells were arrested in G1 phase with α-factor for three hours in Yc-Ura +2% raffinose and the expression of the HO- endonuclease was induced or re-repressed by the addition of 2% galactose or 2% glucose, respectively. Chromatin samples were prepared essentially as described [86]. Slight modifications include: following formalin-mediated crosslinking, cells were resuspended in 4 ml of ChIP buffer [86] and dropped into liquid nitrogen in order to form "popcorn-like" particles. Such frozen cell pellets were then lysed using a SPEX CertiPrep 6850 Freezer Mill to produce deep frozen powdered whole cell extracts. Extracts were thawed on ice and sonicated (30×15 pulses, setting 2, 40% output power) using a Branson Sonifier. H3K4me3 and myc immunoprecipitation were performed using respectively anti-H3K4me3 polyclonal antibody Abcam (Ab8580) and anti-myc antibody Roche (Clone 9E10). Detection of the indicated loci was achieved by PCR using the following primers:

HO cleavage site at mating type = ATTCTTAGCATCA-TTCTTTGTTC and TCCAATCTGTGCACAATGAAG;

CENIV = ATGTTGAAGGAACAGCTGGG and AGGCT-CAATGTTGACTAGCC;

PYK1 = GAAACGATAAGTGCTACTCCGTCCTA and GG-TCATCTATGGGGCTTGAATCT.

Time course HO-cleavage analysis and cleavage efficiency

Cells were grown overnight in Yc-Uracil +2% glycerol lactate medium. Once exponential phase reached, 2% galactose was added and aliquots taken at the specified time points. Cells were then prepared for ChIP analysis or DNA was directly extracted for cleavage efficiency. HO cleavage efficiency was calculated by QPCR using primers listed in Table S2. These primers overlap the cleavage site. Percentage of cleavage was calculated by dividing the number of QPCR amplicons of experimental samples by the number obtained in non-induced cells. Cells grown in glucose (non-induced) were set at a cleavage efficiency of 0%.

Quantitative PCR analyses

For QPCR analyses, specific sequences were amplified by real-time PCR using either a Rotor-Gene RG-3000A or a Rotor-Gene RG-3000 (Corbett Research) and the FastStart SYBR Green Master kit (Roche Applied Sciences). The different primers used are listed in Table S2. Each 10 μl reaction containing 2 μl of DNA sample and 0.3 μM of primers was quantified in triplicate 30 to 45 cycles of 15 s at 94°C, 30 s at 53° to 59°C (Table S2) and 30 s at 72°C.

Supporting Information

Figure S1 Genetic interaction between *BRE2* and the MRX complex. Sensitivity to the radiomimetic drug Bleomycin of strains harbouring deletions of genes encoding COMPASS complex subunits, *BRE2* in (A) and *SPP1* in (B) in combination with a deletion of *RAD50*. Serial ten-fold dilution growth tests of exponentially growing cultures on plates without Bleomycin (YEPD control, left) and with Bleomycin (right) are shown. (C) Western blot analysis of H3K4me2 and H3K4me3 levels in *wt* (LLY33) *set1Δ* (DFY011) *bre2Δ* (BY4741 YLR015W) and *spp1Δ* (BY4741 YPL138C) cells. Pgk1p was used as a loading control.
Found at: doi:10.1371/journal.pgen.1001082.s001 (1.43 MB TIF)

Figure S2 Levels of precise or imprecise NHEJ in *set1*. (Δ. A) Schematic of the gal-HO region flanked by two HO-recognition sites in strain YW1276. Upon cleavage of the indicated sites, NHEJ can occur in a precise fashion which will not recreate the *ADE2* ORF, resulting in red colonies or the *ADE2* orf can be reconstituted by imprecise (+2) NHEJ, yielding white colonies. (B) Overall percentages of precise and imprecise NHEJ as determined in wild type cells *wt* (YW1276), *set1Δ* (DFY021), *yku70Δ* (YW1283) or *dnl4Δ* (DFY022) cells. Note that total surviving colonies (precise plus imprecise NHEJ) in wild-type cells was set to 100% and the fraction of colonies of the respective mutant cells were expressed in relation to that. (C) Genomic HO cleavage efficiency in both *wt* (YW1276) and *set1Δ* (DFY021) cells grown in galactose for 1 hour. (D) HO cleavage efficiency of the cleavage site on plasmid YcpHocut4 of *wt* (DFY027) and *bre1Δ* (DFY028) cells incubated in galactose for the indicated number of hours. Genomic locus hybridization serves as a DNA loading control.
Found at: doi:10.1371/journal.pgen.1001082.s002 (1.11 MB TIF)

Figure S3 Normal levels of homologous recombination in *set1Δ* cells. Analysis of the mating type switching of strains *wt* (DFY046) and *set1Δ* (DFY047). Strains were initially *MAT*a and switched to *MAT*α following induction of the HO cleavage at mating type locus. Appearance of *MAT*α switching product was measured by QPCR using oligos specific for *MAT*α locus. Values were normalized with the amount of switching product found in non-induced samples (glucose) which was set to 1.
Found at: doi:10.1371/journal.pgen.1001082.s003 (0.70 MB TIF)

Figure S4 Variation of histone modification levels after treatment of cells with Phleomycin. Wild type cells ÿLLY33) were exposed to 1, 10 or 100 μg/mL of phleomycin and levels of H3K4me3 and H2AS129P (yeast γ-H2A) were assessed by western blotting. *set1Δ* (DFY021) cells were used as a negative control for H3K4me3 protein modification and Pgk1p was used as a loading control.
Found at: doi:10.1371/journal.pgen.1001082.s004 (0.75 MB TIF)

Figure S5 Mata1 RNA levels do not vary upon treatment of cells with galactose. (A) Northern blot analysis of Mata1 RNA derived from *wt* (DFY027) cells that contain a gal-HO-endonuclease gene on a plasmid and that were grown in glucose or galactose media as indicated. Signals for Mata1 RNA were quantified using a Phosphorimager (Storm) and corrected for loading with using the signals for Act1 mRNA (below). Numbers below each lane indicate the actual ratio if the first lane was set to 1. (B) The same RNA samples as in (A) were used and relative levels quantified by RT-QPCR. RNase treated samples served negative controls. (C) Localization of H3K4me3 to the *MAT* locus in cells harbouring a *MAT*a-inc allele and where the HO site is not cleaved. Cells harbor an integrated copy of the gal-HO gene and were grown either in glucose or in galactose as indicated.
Found at: doi:10.1371/journal.pgen.1001082.s005 (0.82 MB TIF)

Figure S6 Lack of NHEJ components does not sensitize cells to hydroxyurea. Serial ten-fold dilution growth tests of exponentially growing cultures of *wt* (JKM179), *set1Δ* (DFY023), *yku70Δ*

(JKM181), *rad52Δ* (MT0-73) cells on plates with 50 mM hydroxyurea. Colonies were allowed to grow for three days at 30°C.
Found at: doi:10.1371/journal.pgen.1001082.s006 (0.95 MB TIF)

Table S1 Strains used in this study.
Found at: doi:10.1371/journal.pgen.1001082.s007 (0.43 MB RTF)

Table S2 Oligonucleotides used in this study.
Found at: doi:10.1371/journal.pgen.1001082.s008 (0.06 MB RTF)

References

1. Rouse J, Jackson SP (2002) Interfaces between the detection, signaling, and repair of DNA damage. Science 297: 547–551.
2. Evan GI, Vousden KH (2001) Proliferation, cell cycle and apoptosis in cancer. Nature 411: 342–348.
3. Zhou BB, Elledge SJ (2000) The DNA damage response: putting checkpoints in perspective. Nature 408: 433–439.
4. Sanchez Y, Zhou Z, Huang M, Kemp BE, Elledge SJ (1997) Analysis of budding yeast kinases controlled by DNA damage. Methods in Enzymology 283: 398–410.
5. Green CM, Almouzni G (2002) When repair meets chromatin. First in series on chromatin dynamics. EMBO Reports 3: 28–33.
6. Altaf M, Saksouk N, Cote J (2007) Histone modifications in response to DNA damage. Mutation Research 618: 81–90.
7. Osley MA, Tsukuda T, Nickoloff JA (2007) ATP-dependent chromatin remodeling factors and DNA damage repair. Mutation Research 618: 65–80.
8. van Attikum H, Fritsch O, Hohn B, Gasser SM (2004) Recruitment of the INO80 complex by H2A phosphorylation links ATP-dependent chromatin remodeling with DNA double-strand break repair.[see comment]. Cell 119: 777–788.
9. Wurtele H, Verreault A (2006) Histone post-translational modifications and the response to DNA double-strand breaks. Current Opinion in Cell Biology 18: 137–144.
10. van Attikum H, Gasser SM (2005) ATP-dependent chromatin remodeling and DNA double-strand break repair. Cell Cycle 4: 1011–1014.
11. Osley MA, Shen X (2006) Altering nucleosomes during DNA double-strand break repair in yeast. Trends in Genetics 22: 671–677.
12. Fyodorov DV, Kadonaga JT (2001) The many faces of chromatin remodeling: SWItching beyond transcription. Cell 106: 523–525.
13. Shim EY, Ma JL, Oum JH, Yanez Y, Lee SE (2005) The yeast chromatin remodeler RSC complex facilitates end joining repair of DNA double-strand breaks. Molecular & Cellular Biology 25: 3934–3944.
14. Krogan NJ, Keogh MC, Datta N, Sawa C, Ryan OW, et al. (2003) A Snf2 family ATPase complex required for recruitment of the histone H2A variant Htz1. Molecular Cell 12: 1565–1576.
15. Shim EY, Hong SJ, Oum JH, Yanez Y, Zhang Y, et al. (2007) RSC mobilizes nucleosomes to improve accessibility of repair machinery to the damaged chromatin. Molecular & Cellular Biology 27: 1602–1613.
16. Chai B, Huang J, Cairns BR, Laurent BC (2005) Distinct roles for the RSC and Swi/Snf ATP-dependent chromatin remodelers in DNA double-strand break repair. Genes & Development 19: 1656–1661.
17. Papamichos-Chronakis M, Peterson CL (2008) The Ino80 chromatin-remodeling enzyme regulates replisome function and stability.[see comment]. Nature Structural & Molecular Biology 15: 338–345.
18. Morrison AJ, Highland J, Krogan NJ, Arbel-Eden A, Greenblatt JF, et al. (2004) INO80 and gamma-H2AX interaction links ATP-dependent chromatin remodeling to DNA damage repair.[see comment]. Cell 119: 767–775.
19. van Attikum H, Gasser SM (2005) The histone code at DNA breaks: a guide to repair? Nature Reviews Molecular Cell Biology 6: 757–765.
20. Downs JA, Lowndes NF, Jackson SP (2000) A role for Saccharomyces cerevisiae histone H2A in DNA repair. Nature 408: 1001–1004.
21. Weake VM, Workman JL (2008) Histone ubiquitination: triggering gene activity. Mol Cell 29: 653–663.
22. Sun ZW, Allis CD (2002) Ubiquitination of histone H2B regulates H3 methylation and gene silencing in yeast. Nature 418: 104–108.
23. Hwang WW, Venkatasubrahmanyam S, Ianculescu AG, Tong A, Boone C, et al. (2003) A conserved RING finger protein required for histone H2B monoubiquitination and cell size control. Molecular Cell 11: 261–266.
24. Wyce A, Xiao T, Whelan KA, Kosman C, Walter W, et al. (2007) H2B ubiquitylation acts as a barrier to Ctk1 nucleosomal recruitment prior to removal by Ubp8 within a SAGA-related complex. Mol Cell 27: 275–288.
25. Wysocki R, Javaheri A, Allard S, Sha F, Cote J, et al. (2005) Role of Dot1-dependent histone H3 methylation in G1 and S phase DNA damage checkpoint functions of Rad9. Molecular & Cellular Biology 25: 8430–8443.
26. Giannattasio M, Lazzaro F, Plevani P, Muzi-Falconi M (2005) The DNA damage checkpoint response requires histone H2B ubiquitination by Rad6-Bre1 and H3 methylation by Dot1. Journal of Biological Chemistry 280: 9879–9886.
27. Bernstein BE, Humphrey EL, Erlich RL, Schneider R, Bouman P, et al. (2002) Methylation of histone H3 Lys 4 in coding regions of active genes. Proc Natl Acad Sci U S A 99: 8695–8700.
28. Santos-Rosa H, Schneider R, Bannister AJ, Sherriff J, Bernstein BE, et al. (2002) Active genes are tri-methylated at K4 of histone H3. Nature 419: 407–411.
29. Ng HH, Robert F, Young RA, Struhl K (2003) Targeted recruitment of Set1 histone methylase by elongating Pol II provides a localized mark and memory of recent transcriptional activity. Mol Cell 11: 709–719.
30. Ruthenburg AJ, Allis CD, Wysocka J (2007) Methylation of lysine 4 on histone H3: intricacy of writing and reading a single epigenetic mark. Molecular Cell 25: 15–30.
31. Corda Y, Schramke V, Longhese MP, Smokvina T, Paciotti V, et al. (1999) Interaction between Set1p and checkpoint protein Mec3p in DNA repair and telomere functions.[see comment]. Nature Genetics 21: 204–208.
32. Dehe PM, Geli V (2006) The multiple faces of Set1. Biochemistry & Cell Biology 84: 536–548.
33. Tong AH, Evangelista M, Parsons AB, Xu H, Bader GD, et al. (2001) Systematic genetic analysis with ordered arrays of yeast deletion mutants. Science 294: 2364–2368.
34. Ho Y, Gruhler A, Heilbut A, Bader GD, Moore L, et al. (2002) Systematic identification of protein complexes in Saccharomyces cerevisiae by mass spectrometry. Nature 415: 180–183.
35. Wood A, Krogan NJ, Dover J, Schneider J, Heidt J, et al. (2003) Bre1, an E3 ubiquitin ligase required for recruitment and substrate selection of Rad6 at a promoter. Molecular Cell 11: 267–274.
36. Ritchie KB, Mallory JC, Petes TD (1999) Interactions of TLC1 (which encodes the RNA subunit of telomerase), TEL1, and MEC1 in regulating telomere length in the yeast Saccharomyces cerevisiae. Molecular & Cellular Biology 19: 6065–6075.
37. Usui T, Ogawa H, Petrini JH (2001) A DNA damage response pathway controlled by Tel1 and the Mre11 complex. Molecular Cell 7: 1255–1266.
38. Schneider J, Wood A, Lee JS, Schuster R, Dueker J, et al. (2005) Molecular regulation of histone H3 trimethylation by COMPASS and the regulation of gene expression. Mol Cell 19: 849–856.
39. Takahashi YH, Lee JS, Swanson SK, Saraf A, Florens L, et al. (2009) Regulation of H3K4 trimethylation via Cps40 (Spp1) of COMPASS is monoubiquitination independent: implication for a Phe/Tyr switch by the catalytic domain of Set1. Mol Cell Biol 29: 3478–3486.
40. Lee SE, Paques F, Sylvan J, Haber JE (1999) Role of yeast SIR genes and mating type in directing DNA double-strand breaks to homologous and non-homologous repair paths. Current Biology 9: 767–770.
41. Della M, Palmbos PL, Tseng HM, Tonkin LM, Daley JM, et al. (2004) Mycobacterial Ku and ligase proteins constitute a two-component NHEJ repair machine. Science 306: 683–685.
42. Wilson TE (2002) A genomics-based screen for yeast mutants with an altered recombination/end-joining repair ratio. Genetics 162: 677–688.
43. Ma JL, Kim EM, Haber JE, Lee SE (2003) Yeast Mre11 and Rad1 proteins define a Ku-independent mechanism to repair double-strand breaks lacking overlapping end sequences. Mol Cell Biol 23: 8820–8828.
44. Siede W, Friedl AA, Dianova I, Eckardt-Schupp F, Friedberg EC (1996) The Saccharomyces cerevisiae Ku autoantigen homologue affects radiosensitivity only in the absence of homologous recombination. Genetics 142: 91–102.
45. Ng HH, Robert F, Young RA, Struhl K (2002) Genome-wide location and regulated recruitment of the RSC nucleosome-remodeling complex. Genes & Development 16: 806–819.
46. Guenther MG, Levine SS, Boyer LA, Jaenisch R, Young RA (2007) A chromatin landmark and transcription initiation at most promoters in human cells.[see comment]. Cell 130: 77–88.
47. Alcasabas AA, Osborn AJ, Bachant J, Hu F, Werler PJ, et al. (2001) Mrc1 transduces signals of DNA replication stress to activate Rad53. Nature Cell Biology 3: 958–965.

Author Contributions

Conceived and designed the experiments: DF RJW. Performed the experiments: DF. Analyzed the data: DF RJW. Wrote the paper: DF RJW.

48. Osborn AJ, Elledge SJ (2003) Mrc1 is a replication fork component whose phosphorylation in response to DNA replication stress activates Rad53. Genes & Development 17: 1755–1767.

49. Lou H, Komata M, Katou Y, Guan Z, Reis CC, et al. (2008) Mrc1 and DNA polymerase epsilon function together in linking DNA replication and the S phase checkpoint.[see comment]. Molecular Cell 32: 106–117.

50. Szyjka SJ, Viggiani CJ, Aparicio OM (2005) Mrc1 is required for normal progression of replication forks throughout chromatin in S. cerevisiae. Molecular Cell 19: 691–697.

51. Tourriere H, Versini G, Cordon-Preciado V, Alabert C, Pasero P (2005) Mrc1 and Tof1 promote replication fork progression and recovery independently of Rad53. Mol Cell 19: 699–706.

52. Kim J, Daniel J, Espejo A, Lake A, Krishna M, et al. (2006) Tudor, MBT and chromo domains gauge the degree of lysine methylation. EMBO Reports 7: 397–403.

53. Lee JS, Shukla A, Schneider J, Swanson SK, Washburn MP, et al. (2007) Histone crosstalk between H2B monoubiquitination and H3 methylation mediated by COMPASS.[see comment]. Cell 131: 1084–1096.

54. Vitaliano-Prunier A, Menant A, Hobeika M, Geli V, Gwizdek C, et al. (2008) Ubiquitylation of the COMPASS component Swd2 links H2B ubiquitylation to H3K4 trimethylation.[see comment]. Nature Cell Biology 10: 1365–1371.

55. Laribee RN, Krogan NJ, Xiao T, Shibata Y, Hughes TR, et al. (2005) BUR kinase selectively regulates H3 K4 trimethylation and H2B ubiquitylation through recruitment of the PAF elongation complex. Current Biology 15: 1487–1493.

56. Schramke V, Neecke H, Brevet V, Corda Y, Lucchini G, et al. (2001) The set1Delta mutation unveils a novel signaling pathway relayed by the Rad53-dependent hyperphosphorylation of replication protein A that leads to transcriptional activation of repair genes. Genes & Development 15: 1845–1858.

57. Nislow C, Ray E, Pillus L (1997) SET1, a yeast member of the trithorax family, functions in transcriptional silencing and diverse cellular processes. Mol Biol Cell 8: 2421–2436.

58. Zhang K, Lin W, Latham JA, Riefler GM, Schumacher JM, et al. (2005) The Set1 methyltransferase opposes Ipl1 aurora kinase functions in chromosome segregation. Cell 122: 723–734.

59. Borde V, Robine N, Lin W, Bonfils S, Geli V, et al. (2009) Histone H3 lysine 4 trimethylation marks meiotic recombination initiation sites.[see comment]. EMBO Journal 28: 99–111.

60. Sollier J, Lin W, Soustelle C, Suhre K, Nicolas A, et al. (2004) Set1 is required for meiotic S-phase onset, double-strand break formation and middle gene expression. Embo J 23: 1957–1967.

61. Hayashi K, Yoshida K, Matsui Y (2005) A histone H3 methyltransferase controls epigenetic events required for meiotic prophase. Nature 438: 374–378.

62. Chai B, Huang J, Cairns BR, Laurent BC (2005) Distinct roles for the RSC and Swi/Snf ATP-dependent chromatin remodelers in DNA double-strand break repair. Genes Dev 19: 1656–1661.

63. Liang B, Qiu J, Ratnakumar K, Laurent BC (2007) RSC functions as an early double-strand-break sensor in the cell's response to DNA damage. Curr Biol 17: 1432–1437.

64. Tittel-Elmer M, Alabert C, Pasero P, Cobb JA (2009) The MRX complex stabilizes the replisome independently of the S phase checkpoint during replication stress. EMBO J 28: 1142–1156.

65. Roguev A, Bandyopadhyay S, Zofall M, Zhang K, Fischer T, et al. (2008) Conservation and rewiring of functional modules revealed by an epistasis map in fission yeast. Science 322: 405–410.

66. Pena PV, Hom RA, Hung T, Lin H, Kuo AJ, et al. (2008) Histone H3K4me3 binding is required for the DNA repair and apoptotic activities of ING1 tumor suppressor. Journal of Molecular Biology 380: 303–312.

67. Hung T, Binda O, Champagne KS, Kuo AJ, Johnson K, et al. (2009) ING4 mediates crosstalk between histone H3 K4 trimethylation and H3 acetylation to attenuate cellular transformation. Molecular Cell 33: 248–256.

68. Kundu S, Horn PJ, Peterson CL (2007) SWI/SNF is required for transcriptional memory at the yeast GAL gene cluster. Genes & Development 21: 997–1004.

69. Turner BM (2005) Reading signals on the nucleosome with a new nomenclature for modified histones. Nature Structural & Molecular Biology 12: 110–112.

70. Raghuraman MK, Brewer BJ, Fangman WL (1994) Activation of a yeast replication origin near a double-stranded DNA break. Genes & Development 8: 554–562.

71. Tong AH, Lesage G, Bader GD, Ding H, Xu H, et al. (2004) Global mapping of the yeast genetic interaction network.[see comment]. Science 303: 808–813.

72. Alani E, Subbiah S, Kleckner N (1989) The yeast RAD50 gene encodes a predicted 153-kD protein containing a purine nucleotide-binding domain and two large heptad-repeat regions. Genetics 122: 47–57.

73. Briggs SD, Bryk M, Strahl BD, Cheung WL, Davie JK, et al. (2001) Histone H3 lysine 4 methylation is mediated by Set1 and required for cell growth and rDNA silencing in Saccharomyces cerevisiae. Genes & Development 15: 3286–3295.

74. Gietz RD, Schiestl RH, Willems AR, Woods RA (1995) Studies on the transformation of intact yeast cells by the LiAc/SS-DNA/PEG procedure. Yeast 11: 355–360.

75. Brachmann CB, Davies A, Cost GJ, Caputo E, Li J, et al. (1998) Designer deletion strains derived from Saccharomyces cerevisiae S288C: a useful set of strains and plasmids for PCR-mediated gene disruption and other applications. Yeast 14: 115–132.

76. Larrivee M, LeBel C, Wellinger RJ (2004) The generation of proper constitutive G-tails on yeast telomeres is dependent on the MRX complex. Genes & Development 18: 1391–1396.

77. Rose M, Winston F, Hieter P (1990) Methods in yeast genetics: a laboratory course manual. Cold Spring Harbour: Cold Spring Harbour Laboratory Press.

78. Zakian VA, Scott JF (1982) Construction, replication, and chromatin structure of TRP1 RI circle, a multiple-copy synthetic plasmid derived from Saccharomyces cerevisiae chromosomal DNA. Molecular & Cellular Biology 2: 221–232.

79. Wellinger RJ, Wolf AJ, Zakian VA (1993) Structural and temporal analysis of telomere replication in yeast. Cold Spring Harbor Symposia on Quantitative Biology 58: 725–732.

80. Wellinger RJ, Wolf AJ, Zakian VA (1993) Saccharomyces telomeres acquire single-strand TG1-3 tails late in S phase. Cell 72: 51–60.

81. Gravel S, Larrivee M, Labrecque P, Wellinger RJ (1998) Yeast Ku as a regulator of chromosomal DNA end structure. Science 280: 741–744.

82. Toussaint M, Levasseur G, Gervais-Bird J, Wellinger RJ, Elela SA, et al. (2006) A high-throughput method to measure the sensitivity of yeast cells to genotoxic agents in liquid cultures. Mutation Research 606: 92–105.

83. Knop M, Siegers K, Pereira G, Zachariae W, Winsor B, et al. (1999) Epitope tagging of yeast genes using a PCR-based strategy: more tags and improved practical routines. Yeast 15: 963–972.

84. Sambrook J, Fritsch EF, Maniatis T (1989) Molecular Cloning: A Laboratory Manual, Second Edition. Cold Spring Harbor, New York: Cold Spring Harbor Laboratory Press.

85. Larose S, Laterreur N, Ghazal G, Gagnon J, Wellinger RJ, et al. (2007) RNase III-dependent regulation of yeast telomerase. Journal of Biological Chemistry 282: 4373–4381.

86. Vodenicharov MD, Wellinger RJ (2006) DNA degradation at unprotected telomeres in yeast is regulated by the CDK1 (Cdc28/Clb) cell-cycle kinase. Molecular Cell 24: 127–137.